



LAWRENCE  
LIVERMORE  
NATIONAL  
LABORATORY

# Mono and Multivalency In Tethered Protein-Carbohydrate Bonds

T. V. Ratto, K. C. Langry, R. E. Rudd, R. L.  
Balhorn, M. W. McElfresh

February 2, 2004

Biophysical Society Meeting  
Baltimore, MD, United States  
February 14, 2004 through February 18, 2004

## **Disclaimer**

---

This document was prepared as an account of work sponsored by an agency of the United States Government. Neither the United States Government nor the University of California nor any of their employees, makes any warranty, express or implied, or assumes any legal liability or responsibility for the accuracy, completeness, or usefulness of any information, apparatus, product, or process disclosed, or represents that its use would not infringe privately owned rights. Reference herein to any specific commercial product, process, or service by trade name, trademark, manufacturer, or otherwise, does not necessarily constitute or imply its endorsement, recommendation, or favoring by the United States Government or the University of California. The views and opinions of authors expressed herein do not necessarily state or reflect those of the United States Government or the University of California, and shall not be used for advertising or product endorsement purposes.

# Mono and Multivalency In Tethered Protein-Carbohydrate Bonds

UCRL-CONF-202145

Timothy V. Ratto<sup>1</sup>, Kevin C. Langry<sup>1</sup>, Robert E. Rudd<sup>2</sup>, Rodney L. Balhorn<sup>3</sup>, and Michael W. McElfresh<sup>1</sup>

1- Chemistry and Materials Science, Lawrence Livermore National Laboratory, L-418, 7000 East Ave. Livermore, CA 94550

2- Physics and Advanced Technologies, Lawrence Livermore National Laboratory, L-045, 7000 East Ave. Livermore, CA 94550

3- Biology and Biotechnology Research Program, Lawrence Livermore National Laboratory, L-452, 7000 East Ave. Livermore, CA 94550.

## INTRODUCTION

Molecular recognition in biological systems typically involves large numbers of interactions simultaneously. By using a multivalent approach, weak interactions with fairly low specificity can become strong highly specific interactions. Additionally, this allows an organism to control the strength and specificity of an interaction simply by controlling the number of binding molecules (or binding sites), which in turn can be controlled through transcriptional regulation.

Force spectroscopy has recently emerged as a powerful technique for measuring binding properties of biological interactions at the single molecule level (Zlatanova et al., 2000; Chen and Moy, 2002). This non-imaging mode utilizes biological molecules attached to an AFM (Atomic Force Microscopy) cantilever, which is then used to probe an either naturally, as with cell membranes, or artificially, ligand-functionalized surface. The AFM cantilever is moved close enough to the surface for the molecules to bind and then retracted at a constant velocity. By monitoring the deflection of the cantilever during the approach-retraction cycle the extension length and bond rupture force can be ascertained (Liu et al., 1999; Benoit et al., 2000; Clausen-Schaumann et al., 2000; Conti et al., 2002; Florin et al., 1994; Hugel and Seitz, 2001; Ludwig et al., 1994; Merkel, 2001). Attaching the binding species with polymer tethers and correlating bond rupture with the distance the polymer is stretched prior to rupture also allows the differentiation of specific from non-specific bond formation (Riener et al., 2003) and, in conjunction with computer simulations, can provide information about the molecular configurations (e.g. protein number and tether length) of both the probe and the sample surface. Previous investigations utilizing tethered molecules have focused mainly on a more qualitative discussion of the effects on the force curve due to the tether, such as allowing oriented coupling due to the increased mobility of the protein, and separating specific interactions from nonspecific tip-substrate adhesion. Here we present an in-depth quantitative analysis of the effects due to the presence of the tethers.

In this study, we investigate the bond rupture force between ConcanavalinA (ConA) and mannose. ConA is a lectin, or carbohydrate-binding protein, and has been well-characterized using crystallography and other methods (Mann et al., 1998; McDonnell, 2001; Kanellopoulos et al., 1996). Carbohydrate binding serves as the initial step in a wide variety of biological functions, ranging from fertilization to viral infection (Varki, 1993) and expanding the understanding of the mechanisms behind carbohydrate recognition will assist in the development of new strategies for understanding biological function and combating disease. Additionally, the valency of ConA can be controlled by pH and thus serves as an admirable system for studying multivalency in protein-carbohydrate interactions.

## EXPERIMENTAL

**Tip Functionalization.** New silicon nitride cantilevers stored under nitrogen were used without additional cleaning. Cantilevers were silanized from the vapor phase using recently distilled 3-

aminopropyl-triethoxysilane (APTES) and methyltriethoxysilane (MTES) at an amino to methyl ratio of 1/250 in order to reduce the number of active groups on the tip. The tips were then immersed for 30 minutes in chloroform containing 10 mg/mL of a,w-diNHS-poly(ethylene glycol) (PEG) with a nominal molecular weight of 3400 amu (PEG-(SPA)2, 4M4M0F02, Shearwater Polymers, Huntsville, AL now Nektar Therapeutics, www.nektar.com), corresponding to a nominal extended length of approximately 25 nm. The tips were rinsed with chloroform, dried with nitrogen and immediately immersed in 25 mM phosphate buffer solution, pH 8.0, containing 2 mg/mL ConA (Canavalia ensiformis, Jack bean, Type VI, Sigma). After 20 minutes, the tips were removed and rinsed briefly with 25 mM phosphate buffer, pH 8, and then for 10 minutes with three volumes of 25 mM phosphate buffer, pH 5.0. Since ConA is a dimer below pH 7 this step is necessary in order to remove the tetrameric form of ConA, as well as any larger aggregates. For studies requiring multivalent ConA, the buffer pH was maintained at 7.4 or above. The derivatized tips were used within several hours of their preparation.

**Substrate Functionalization.** Ethanol-rinsed gold-coated (Au thickness 1000 Å) silicon (Platypus Technologies, LLC, www.platypustech.com) was immersed in ethanol containing 1 mM 16-mercaptohexadecanoic acid for 30 minutes. The resulting self-assembled monolayers (SAMs) were rinsed first with ethanol and then with four volumes of chloroform. The SAMs were then immersed in chloroform containing 10mg/mL 1,1'-carbonyldiimidazole for 30 minutes and then immediately rinsed in four volumes of chloroform before being immersed in chloroform containing 10 mg/mL of a,w-diamino-polyethylene glycol with a nominal molecular weight of 3400 amu (PEG-(amine)2, 2V2V0F22, Shearwater Polymers). The SAMs were rinsed in four volumes of chloroform, dried with nitrogen, and immersed for one hour in dimethylformamide containing 6 mg/mL a-D-mannopyranosylphenyl isothiocyanate (Sigma) under an atmosphere of dry nitrogen. The SAMs were rinsed sequentially with ethanol, water, and ethanol and dried with nitrogen. The derivatized SAMs were used within hours of their preparation.

All points of attachment between the protein and the tip and the ligand and the substrate consist of covalent bonds. At bond loading rates comparable to the rates we use in this study, covalent attachments have bond rupture forces in excess of 1000 pN (Grandbois et al., 1999), thus we can be confident that the rupture forces we measure are not due to the polymer tethers being removed from either the tip or the substrate.

## RESULTS AND DISCUSSION

**Rupture Distances.** AFM direct force measurements were acquired to characterize both the strength of the adhesive interactions between the polymer-tethered dimeric ConA protein and the mannose functionalized substrate, and the bond rupture distance at which the interactions took place. We found adhesive interactions clustering at three characteristic length scales, less than 10 nm, between 10 and 33 nm, and between 33 and 43 nm, as shown in Fig. 1, in comparison with the nominal PEG length of 25 nm. Figure 1A shows a representative interaction occurring close to the point of contact between the AFM tip and the substrate, Fig. 1B shows an additional interaction at a tip-substrate distance of ~20 nm, and Fig. 1C shows an additional interaction at a tip-substrate distance of ~40 nm. This latter interaction at about twice the PEG length is the proposed specific interaction between the tethered ConA and the tethered mannose, as depicted in the schematic diagram in Fig. 1.

**Bond Rupture Forces.** Histograms of the frequencies of adhesive interactions at tip-substrate distances between 1 and 50 nm for a ConA functionalized tip on a mannose functionalized substrate are shown in Fig. 2A. The same data are graphed as the rupture force vs. tip-substrate distance in Fig. 2C to show how the rupture forces are clustered as a function of tip-substrate distance. We find that the most frequent rupture force for the ConA- mannose bond is  $47 \pm 9$  pN at a bond loading rate of ~10 nN/s. We believe this to be the rupture force for a single ConA-mannose interaction- although the protein is a dimer - as multiples of this force (e.g. double) are not seen at this pH. Possibly the attachment of the polymer tether interferes with bond

formation at one of the binding sites of the ConA dimer. In order to demonstrate that the observed adhesive interactions seen between 33 and 43 nm are indeed due to specific ConA-mannose bond rupture, we replaced the working buffer with buffer containing 5 mM  $\alpha$ -D-mannose, known to be a competitive inhibitor of ConA. Competitive inhibition of binding is commonly used as an indicator of protein-ligand specificity. The adhesive interactions between 33 and 43 nm were almost completely eliminated by the presence of the blocking agent while the interactions below 33 nm were mostly unaffected (See Figs. 2B and 2D).

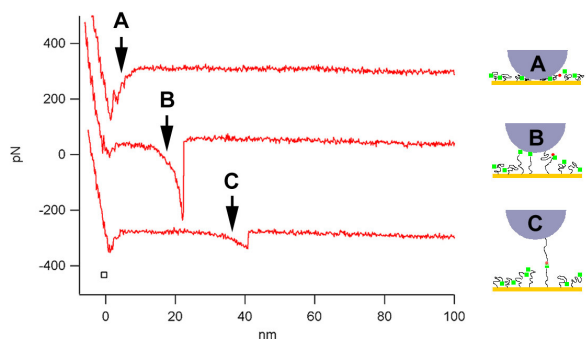


**Figure 1.** Experimental AFM retraction curves and schematics showing interactions at three characteristic distances, A, proposed non-specific tip-substrate interactions (< 10 nm), B, proposed non-specific tip-ligand interactions (between 10 and 33 nm), and C, proposed specific protein-ligand interactions (between 33 and 43 nm). Note that the zero point along the x-axis denotes the point of contact between the tip and the substrate. Force curves A and C have been offset in the y-axis in order to fit all three curves on one graph. (Ratto, submitted)

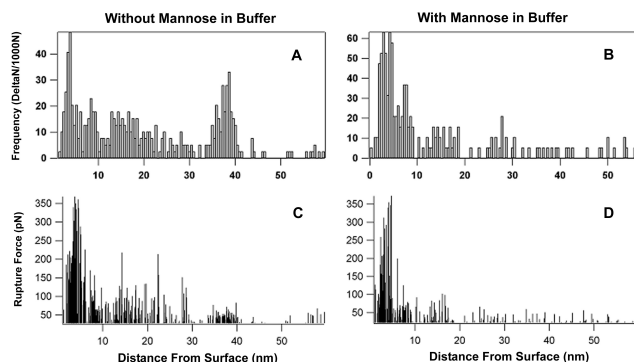


**Figure 2.** Histograms of the frequency of interactions (Figs. A and B) and magnitude of the rupture forces (Figs. C and D) at increasing distances from the point of contact between the AFM tip and the surface. Fig. A and C show the specific interactions between the ConA and mannose at the characteristic lengths between 33 and 43 nm. When the buffer solution in the AFM liquid cell is exchanged with buffer containing free mannose, binding between the ConA on the AFM tip and the mannose attached to the substrate is blocked, and the specific interactions seen at the characteristic lengths between 33 and 43 nm can no longer be seen (Figs. B and D). Note that the number of interactions at lengths less than 33 nm also decreases upon addition of free mannose implying that specific interactions may also occur at these lengths. These may be due to the tethered protein adhering to the AFM tip or tethered ligands adhering to the substrate prior to the formation of a bond. (Ratto, submitted)

Several features of the large cluster of interactions between 33 and 43 nm seen in Fig. 2A indicate these rupture forces correspond to the breaking of specific protein-carbohydrate bonds that form between a single tethered protein on the tip and the tethered ligands on the

substrate. First, the interactions are clustered around 40 nm, greater than the length of a single tether but less than the additive length of two tethers. Second, this cluster was not seen in either the experiment in which the ConA-mannose interaction was blocked by the addition of free mannose into the buffer solution (Fig. 2C) or when an unfunctionalized tip was used to probe the substrate. The width of the cluster of interactions can be directly attributed to the 10 nm wide distribution of polymer lengths as measured by MALDI (Matrix Assisted Laser Desorption Spectroscopy, data not shown), which is representative of the length distribution of the polymer-tethered ligands on the substrate. Finally, the rupture forces for the interactions between 33 and 43 nm are clustered around  $47 \pm 9$  pN (Fig. 3A), while the rupture forces for the interactions between 5 and 33 nm show a much broader distribution of values, ranging from around 30 to 160 pN (See Figs. 3B and 3C). Thus, we can state with some certainty that the fraction of measurements represented by the 33-43 nm cluster consists of specific bonding events between a single ConA and mannose, however, there may be other specific bonding events that lie outside the cluster.

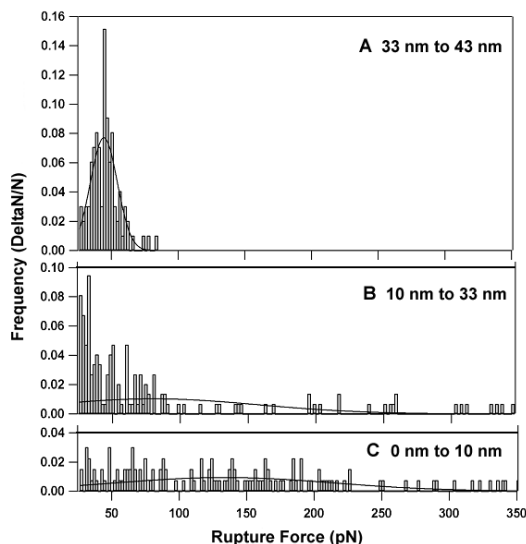


**Figure 3.** Frequency vs. force histograms showing the distribution of forces from the three characteristic regions (sorted by length) of the force curves. Figure A shows the distribution of forces measured between 33 and 43 nm from the point of contact between the tip and substrate. A Gaussian best fit to the histogram reveals the proposed single molecule most frequent rupture force for the ConA-mannose interaction of  $47 \pm 9$  pN. The distributions of forces for the other two length scales are much broader, varying between approximately 20 and 350 pN. Note that these forces were measured at bond loading rates of 100 nm/second. (Ratto, submitted)

**Multivalency.** In order to increase the probability of multivalent interactions, tips were functionalized with ConA at a pH of 7.4 or higher (above pH ~7 ConA is a tetramer, or higher-order protein aggregate.) When force spectroscopy was used to measure the adhesive interaction between multimeric ConA and the mannose-functionalized substrate, the width of the force distribution broadened in comparison to the previous result (Fig. 4). Although a peak remained close to the previously measured value of ~50 pN, higher forces were also measured indicating that multivalent bonds were being ruptured. In addition to the increase in the width of the force distribution, the distance width of the cluster of interactions corresponding to the specific bond rupture also increased. As previously shown (Fig. 2,) when the monomeric form of the protein was used, the specific interactions were clustered between 33 and 43 nm. When multimeric ConA was used, however, the interactions were clustered between 36 and 50 nm from the tip-substrate contact point.

We reasoned that due to variances in tip functionalization the location of the specific bond cluster could vary, however, the width of the cluster should continue to correspond with the 10 nm wide distribution of polymer lengths (measured with MALDI, data not shown) present on the substrate. We reasoned that perhaps there were additional tethered proteins on the tip that were contributing to the increase in the force distribution and cluster widths. If there were multiple tethers on the tip, we should have seen multiple interactions at least occasionally in the force curves. This was not the case however, as each curve only showed a single interaction between 36 and 53 nm. In an attempt to unravel the mystery, we graphed the rupture force as a function of the rupture location (Fig. 5.) This revealed that the weaker rupture forces tended to occur earlier, or rather at smaller distances. In fact, it appeared that on average the weaker ruptures occurred at around 40nm, while the stronger bonds ruptured at about 44 nm. We hypothesized that since the distance a polymer chain stretches is directly dependent on the force applied to the chain, the stronger bonds were perhaps stretching the polymer tethers further before the bonds ruptured. In order to evaluate whether the higher forces that we measured were correlated with the increased distances, we used the Worm-Like Chain model (WLC) to simulate force spectroscopy data. The WLC has been shown to accurately predict the behavior of PEG polymer chains under applied forces. According to the WLC, for a 54 nm polymer chain (approximately double our nominal tether length) the application of 50pN of force corresponds to an additional 4 nm stretch. This result adds additional evidence to support the idea that multivalency can result in detectable differences in force rupture distances measured by force spectroscopy experiments and may serve as a tool for detecting multivalent interactions between biological macromolecules.

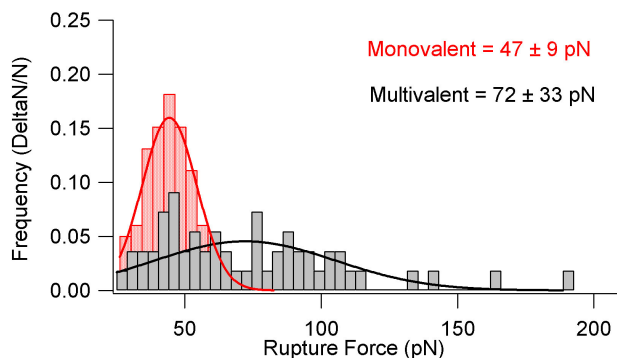


**Figure 4.** Frequency versus force histograms comparing the monovalent bond rupture force ( $47 \pm 9$  pN) with the multivalent interaction ( $72 \pm 33$  pN). The broadening of the rupture force distribution also correlates with an increase in the specific bond cluster width (data not shown.)

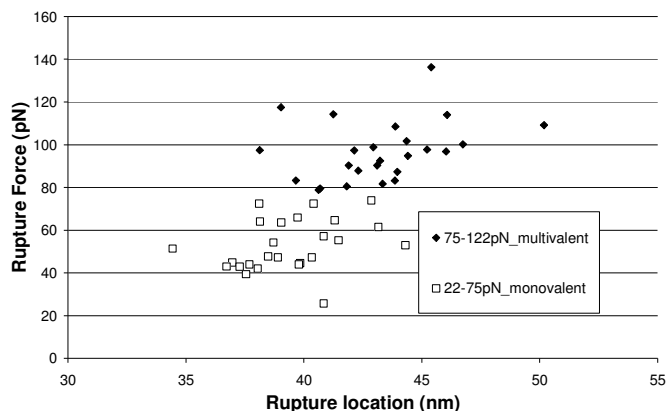


**Figure 5.** Rupture force as a function of the rupture location (the point at which the bond ruptures relative to the tip-substrate contact point). Note that weaker bonds rupture at smaller distances.

## ACKNOWLEDGMENTS

We would like to thank Stuart Lindsey, Christine Orme, and Aleksandr Noy for useful discussions, Sharon Shields and Julio Camarero for mass spectrometry assistance, and Sal Zepeda and Scott McCall for assistance with data analysis. This work was performed under the auspices of the US Dept. of Energy by the Univ. of California/Lawrence Livermore National Laboratory under Contract No. W-7405-Eng-48.

## REFERENCES

1. Benoit, M.; Gabriel, D.; Gerisch, G.; Gaub, H. E. *Nature Cell Biology* **2000**, *2*, 313-317.
2. Chen, A. L.; Moy, V. T. *Atomic Force Microscopy in Cell Biology* **2002**, *68*, 301-309.
3. Clausen-Schaumann, H.; Seitz, M.; Krautbauer, R.; Gaub, H. E. *Current Opinion in Chemical Biology* **2000**, *4*, 524-530.
4. Conti, M.; Donati, G.; Cianciolo, G.; Stefoni, S.; Samori, B. *Journal of Biomedical Materials Research* **2002**, *61*, 370-379.
5. Florin, E. L.; Moy, V. T.; Gaub, H. E. *Science* **1994**, *264*, 415-417.
6. Hugel, T.; Seitz, M. *Macromolecular Rapid Communications* **2001**, *22*, 989-1016.
7. Kanellopoulos, P. N.; Tucker, P. A.; Pavlou, K.; Agianian, B.; Hamodrakas, S. J. *Journal of Structural Biology* **1996**, *117*, 16-23.
8. Liu, Y. Z.; Leuba, S. H.; Lindsay, S. M. *Langmuir* **1999**, *15*, 8547-8548.
9. Ludwig, M.; Moy, V. T.; Rief, M.; Florin, E. L.; Gaub, H. E. *Microscopy Microanalysis Microstructures* **1994**, *5*, 321-328.
10. Mann, D. A.; Kanai, M.; Maly, D. J.; Kiessling, L. L. *Journal of the American Chemical Society* **1998**, *120*, 10575-10582.
11. McDonnell, J. M. *Current Opinion in Chemical Biology* **2001**, *5*, 572-577.
12. Merkel, R. *Physics Reports-Review Section of Physics Letters* **2001**, *346*, 344-385.
13. Ratto, T. V.; Langry, K.; Rudd, R. E.; Balhorn, R.; Allen, M. J.; McElfresh, M. *Biophysical Journal* **Submitted**.
14. Riener, C. K.; Stroh, C. M.; Ebner, A.; Klampfl, C.; Gall, A. A.; Romanin, C.; Lyubchenko, Y. L.; Hinterdorfer, P.; Gruber, H. J. *Analytica Chimica Acta* **2003**, *479*, 59-75.
15. Varki, A. *Glycobiology* **1993**, *3*, 97-130.